Modulation of Density and Orientation of Amphiphilic DNA on Phospholipid Membranes. II. Vesicles

Martina Banchelli,[†] Filippo Gambinossi,[†] Adeline Durand,[‡] Gabriella Caminati,[†] Tom Brown,[‡] Debora Berti,*[,†] and Piero Baglioni*[,†]

Department of Chemistry and CSGI, University of Florence, via della Lastruccia 3 - Sesto Fiorentino, 50019 Florence, Italy, and School of Chemistry, University of Southampton, SO17 1BJ, Southampton, United Kingdom

Received: January 25, 2010; Revised Manuscript Received: April 16, 2010

In the present series of papers, we describe the results of a systematic study on the anchoring of cholesterol-tagged oligonucleotides to phospholipid bilayers followed by membrane-assisted hybridization of the complementary strand in solution. This paper compares the behavior of two cholesteryl modified oligonucleotides, differing in the architecture and hydrophobicity of the lipophilic moiety, in the self-aggregation, hybridization, and insertion in phospholipid vesicle membranes. We have focused our attention on a singly substituted derivative (SC-ON_1) and a multicholesterol (MC-ON_1) derivative, where the cholesteryl units are inserted at the desired positions along a noncoupling T-sequence. The self-aggregation properties in solution are also explicitly taken into account and evaluated as competitive with respect to the adsorption at fluid or solid interfaces and to hybridization with the complementary ON_2 sequence. By exploring a wide range of ON derivative concentrations, different peculiar scenarios emerge for different hydrophobicity of the amphiphilic DNA guest molecules on the vesicles, in terms of distribution and conformation of the single strand and consequent coupling properties with the complementary strand in solution.

Introduction

DNA-based soft nanotechnology uses nucleic building blocks for the directed self-assembly into nanometer-scaled objects with defined structural and functional properties, predetermined through the sequence choice and encoded by selective base pairing.[1−4]

To further extend the range of application of DNA-directed construction of nanomaterials, the grafting of single-strand DNA derivatives on surfaces or nano-objects, such as hard nanoparticles,[5,6] or noncovalent insertion in amphiphilic aggregates,[7−9] such as phospholipid bilayers, has been explored. These latter soft hybrid nanomaterials combine the characteristics of amphiphilic self-assembly, in terms of ease of preparation, responsiveness with the unique features offered by DNA structural fidelity, and coupling specificity, enabling further hierarchical aggregation in functional arrays of nanounits. Our group has recently studied the incorporation of a cholesteryl-tetraethyleneglycol functionalized oligonucleotide (Chol-TEG-2′, hereafter called SC-ON_1) in phospholipid vesicles[10] and its hybridization with a complementary strand. The results have been interpreted in terms of average distance between noncovalent grafting sites onto the membrane. Both the oligonucleotide conformation and the hybridization kinetics are strongly dependent on macromolecular crowding at the liposomal surface. A remarkable result was the fact that above a critical grafting density, connected to the lipophilic oligonucleotide excluded area, coupling kinetics are slowed down relative to strand pairing in solution. Conversely, when the average interoligonucleotide density on the liposomal surface is low, coupling is faster than in bulk medium.

DNA amphiphiles incorporated in lipid vesicles have also been used as molecular zippers to model ligand-mediated vesicle docking and fusion[11] or alternatively to build vesicle-based nanocontainer layers on layer-by-layer particles.[12] Very recently, the possibility of creating Janus-like vesicles with coexisting lipid domains where amphiphilic DNA molecules can preferentially partition has been shown: these sticky patches would break the spherical symmetry of intervesicle interactions, opening up the possibility of directional vesicle adhesion.[13]

A yet unexplored application, beyond the use of DNA as a coupling agent between soft colloidal objects, is the construction of extended DNA networks, lattices, or nanomachines supported onto soft surfaces to position electronically or optically active components through sequence-specific binding with subnanometer precision.[14] To this aim, we have recently investigated the aggregation in solution of linear ss-42-mer oligonucleotides, demonstrating their self-assembly into pseudohexagonal DNA subunits, intended to be the elementary cells of a pseudohexagonal network with rigid sides.[15] These results have been extended to the construction of a lipid membrane/pseudohexagonal DNA hybrid, anchored on the membrane through to the cholesteryl-TEG functionalization of the first strand. The effects of grafting density, lipid/DNA ratio, liposome number density, and preparation procedure on the final structure and yield of the resulting hybrid nanomaterial were demonstrated.[16] This work was the first example of realization of nonlinear DNA constructs onto fluid membranes. Remarkably, closely matching results for the thickness of the DNA layer have been obtained for DNA adsorption on liposomes and on SLB at the same grafting density.

These few examples nicely illustrate the diversity of long-term goals that can be envisioned thanks to the use of DNA decorated vesicles, both in the biomedical field (modeling of

* Corresponding authors. Piero Baglioni. Phone: +39 055-457-3033. Fax: +39 055-457-3032. E-mail: piero.baglioni@unifi.it. Debora Berti. Phone: +39 055-457-3038. Fax: +39 055-457-3032. E-mail: berti@csgi.unifi.it.
† University of Florence.
‡ University of Southampton.

10.1021/jp100731c
Published on Web 05/06/2010

ligand−receptor mediated events, drug delivery, etc.) and in DNA-based nanotechnology. This rapidly growing field calls for a deeper understanding of DNA−membrane hybrids on fundamental grounds to highlight the structural determinants that ultimately drive the functional properties of these "smart" nanostructures.

The structural and functional robustness of DNA/membrane hybrids relies on the initial choice of the membrane-anchoring oligonucleotide. Several aspects remain to be addressed in the molecular design of the lipophilic oligonucleotide that, once inserted into the membrane, recruits the complementary oligonucleotides. The conjugation of different hydrophobic groups to one of the ends of a single-stranded nucleic acid imparts amphiphilicity to DNA and allows the molecule to be adsorbed and oriented at fluid surfaces, as illustrated in the introduction of the accompanying paper and in recent reviews.[17] These hydrophobic oligonucleotides must show robust affinity toward the lipid membrane and at the same time display high pairing fidelity and yield with the complementary soluble strands, both from a thermodynamic and from a kinetic point of view. The parameters that can be varied are the nature, the number, and the relative positioning of the hydrophobic units. Fine-tuning can be further pursued with a hydrophilic linker (usually an oligoethyleneglycol) that separates the lipophilic moiety from the oligonucleotide.

A possible design principle to improve bilayer partition is to increase the hydrophobicity of the membrane anchor, but this in turn affects the presence, size, shape, and dynamics of self-aggregates in solution, which may prevent efficient partition in bilayer membranes. This aspect is often scarcely appreciated or even neglected; however, depending on the architecture of the hydrophobic tag of the oligonucleotides, and on the dynamic feature of the self-aggregates, it can have a dramatic impact on bilayer partition and on the mechanism of insertion.

We have focused our attention on the hydrophobic architecture of the oligonucleotide anchor, comparing two cholesteryl modified oligonucleotides, with a different hydrophobic architecture: a singly substituted one (SC-ON_1), already partially characterized,[10] and a multicholesterol (MC-ON_1) derivative, where the cholesteryl units are positioned at the desired position along a noncoupling T-sequence. The incorporation in planar supported bilayers and coupling with the complementary oligonucleotide have been investigated through QCM-Z techniques and reported in the first part of this series of manuscripts,[18] revealing that the presence of multiple cholesterol units is not a mere enhancer of hydrophobicity but rather radically changes the mechanism of adsorption at the interface. If a planar supported lipid bilayer of POPC is equilibrated with increasing SC-ON_1 or MC-ON_1 concentrations, a totally different behavior emerges: in the monolayer saturation regime, the application of a mean-field Bragg−Williams (BW) approximation with nearest-neighbor interactions revealed a pseudo-Langmuir behavior for SC-ON_1, while strong mutual interactions were observed for MC-ON_1, resulting in a high cooperative process. Moreover, while for SC-ON_1 the bilayer coverage with a monolayer results in saturation, for MC-ON_1 two other regimes can be distinguished. Thanks to the presence of multiple cholesterol units, the monomers can approach the interface and be absorbed onto the first layer due to hydrophobic interactions with possibly dangling cholesteryl units.

The aim of the present contribution is to extend this previous investigation, reporting on the incorporation and hybridization properties of cholesterol-modified oligonucleotides in unilamellar phospholipid vesicles. The self-aggregation properties in solution are also explicitly taken into account and evaluated as a competitive and/or adsorption determining event with respect to the adsorption at fluid or solid interfaces and to hybridization with the complementary ON_2 sequence.[19]

The comparison of complementary information through classical solution techniques with the behavior in SLB, thoroughly characterized from QCM-Z studies, allows us to possibly verify the effect of the curvature on the formation of the DNA/lipid hybrid, as far as the choice of the hydrophobic anchoring unit is concerned. This will allow us to extend our understanding of planar bilayer/DNA hybrids to monodisperse and size-tunable closed bilayers with DNA decoration, more suited for the design of hierarchical hybrid assemblies directed by base pairing.

The results are presented as follows: first, the self-aggregation of SC-ON_1 and of MC-ON_1 is investigated and compared through fluorescence, light scattering, and surface tension measurements; then, the structural properties of the aggregates in solution are discussed, based on dynamic light scattering results and excimer emission properties of the pyrene probe. Adsorption on liposomes in the different regimes of aggregation are presented and compared in terms of added hydrodynamic thickness. Duplex formation and thermal disassembly are then addressed. Finally, the results obtained for planar bilayers and their implications are discussed.

Materials and Methods

Materials. Oligonucleotide synthesis was carried out on automated DNA synthesizers (Applied Biosystems ABI 394) through the phosphoramidite method, as described elsewhere.[20] The SC-ON_1 structure and the MC-ON_1 structures are shown in Figure 1. The molecular structures of SC-ON_1 and MC-ON_1 are shown in Figure 1; an estimation of the hydrodynamic molecular sizes for the dry macromolecules, performed by means of the HYDROPRO program on an in vacuo optimized molecular geometry, yields hydrodynamic radii of 2.2 and 3.3 nm for the unimers, respectively. SC-ON_1 and MC-ON_1 have 1 and an average of 3.5 cholesteryl groups per molecule, respectively. For MC-ON_1 these hydrophobic groups are distributed along a noncoupling 13 T sequence. Two of these units are separated only by one unmodified thymine and are therefore in close contact. The other units are separated by sequences of three thymine bases, which act as joints and should provide sufficient conformational flexibility.

The complementary oligonucleotide ON_2FAM used for the hybridization experiments was obtained by adding the fluorescein phosphoramidite monomer to the 5′ end of the oligonucleotide CTGAAATTATGATAAAGA.

Liposome Preparation. POPC vesicles were prepared by evaporation of the solvent from a choloroform/methanol solution of the lipid; the dry lipidic film was solvated by addition of a 50 mM TRIS, 100 mM NaCl solution (TBS) with pH: 7.5. The suspension was vortexed, frozen−thawed (liquid nitrogen) six times, and sized down by repeated extrusion (Extruder by Lipex Biomembranes Inc., Vancouver, Canada) through stacks of Nucleopore polycarbonate membranes[21] (200, 100, and 50 nm pore size), yielding a narrow sized distribution of unilamellar vesicles. Different liposomal preparations resulted in slightly different initial sizes and hydrodynamic radii ranging from 33 to 35 nm. The total membrane area and the number of lipid molecules in the outer leaflet were determined from the hydrodynamic radius considering an area per POPC of 0.70 nm^2 and a membrane thickness of 4 nm for the bilayer in the liquid crystalline state, respectively. The vesicular dispersion was then diluted to 1.3 mM with solutions of cholesteryl-oligonucleotide

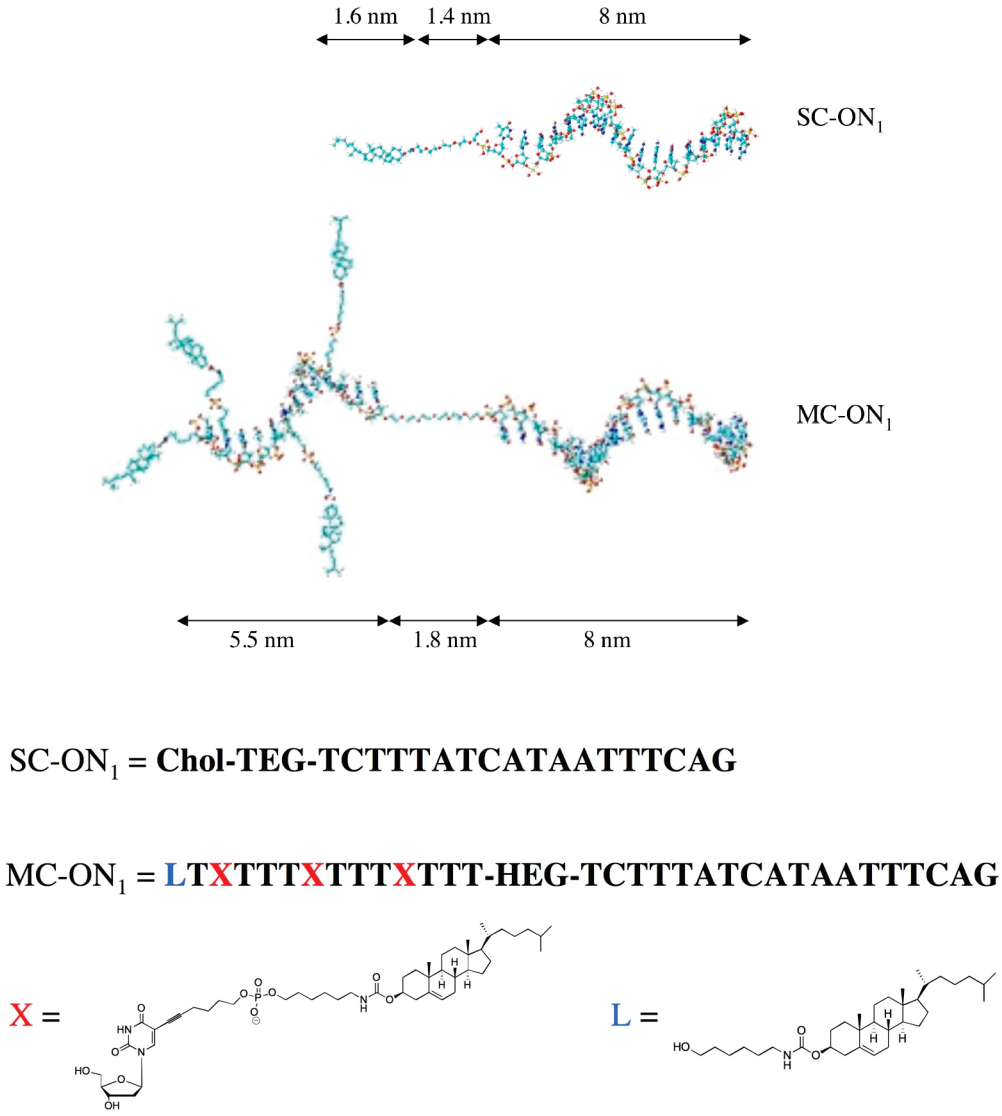

Figure 1. Molecular structure of SC-ON$_1$ and MC-ON$_1$ optimized with Hyperchem in vacuo and chemical formulas.

in TRIS buffer saline (Tris 50 mM, NaCl 100 mM, pH 7.5, TBS), at different oligonucleotide concentrations.

Experimental Methods

Fluorescence. Steady state fluorescence was measured with a LS50B spectrofluorimeter (Perkin-Elmer, Italy). The fluorescence emission spectra of pyrene were recorded in the corrected spectrum mode, between 350 and 500 nm with an excitation wavelength of 335 and 2.5 nm slit, and at least 10 scans were averaged for each spectrum. Pyrene concentration was 1 μM in all samples. The ratio of the intensities I_1/I_3 of Py fluorescence emission, determined from the first (372 nm) and the third (382 nm) vibronic peaks of the emission spectrum, was evaluated for different amphiphilic DNA concentrations.

Py excimer formation, revealed by an increased emission intensity at 480 nm, was also monitored to provide information about the size and the number of aggregates.[22]

Quasi Elastic Light Scattering (QELS). QELS experiments were carried out with a Brookhaven Instrument: BI 9000AT correlator card and BI 200SM goniometer (New York, USA). The signal was detected by an EMI 9863B/350 photomultiplier. The light source was the doubled frequency of a Coherent Innova diode pumped Nd:YAG laser, $\lambda = 532$ nm, 20 mW. The long-term power stability of the laser was $\pm 0.5\%$. Self-beating detection was recorded using decahydronaphthalene (thermostatted by a water circulating system) as index matching liquid. A temperature probe was inserted in the sample to monitor T while simultaneously recording autocorrelation functions. For each sample, at least three separate measurements were performed, and then the average function was taken for data analysis.

In dynamic light scattering experiments, the normalized time autocorrelation function of the intensity of the scattered light is measured. It can be expressed as

$$g_2(q,t) = \frac{\langle I(q,t)I(q,0)\rangle}{I(q,0)I(q,0)} = A[1 + \beta|g_1(q,t)|^2] \qquad (1)$$

where A is the measured baseline; β is the spatial coherence factor; and $g_1(q,t)$ is the normalized electric field correlation function.

For a dilute suspension of monodisperse particles, $g_1(q,t)$ decays exponentially with a decay rate $\Gamma = Dq^2$, where q is the magnitude of the scattering wave vector and D is the translational diffusion coefficient, which is related to the hydrodynamic diameter through the Debye−Stokes−Einstein relationship

$$D = \frac{k_B T}{6\pi\eta R_h} \quad (2)$$

with k_BT being the thermal energy and η the viscosity of the aqueous phase. For a dilute suspension of polydisperse particles, the correlation function $g_1(q,t)$ no longer has a single exponential decay and can be written as the Laplace transform of a continuous distribution $G(\Gamma)$ of decay times

$$g_1(t) = \int_0^\infty G(\Gamma)\exp(-\Gamma t)d\Gamma \quad (3)$$

The analysis of the decay time distribution has been carried out by the inverse Laplace transformation by means of the CONTIN method.[23]

UV−vis Spectrophotometry. UV−vis spectra were recorded with a Lambda 900 spectrophotometer (Perkin-Elmer, Italy) and a Cary 100 spectrometer (Varian, Italy). Thermal cycles from 10 to 80 °C were performed at 0.5 °C/min.

Surface Tension. The air−water surface tension was measured through drop shape analysis with a drop pendant shape apparatus from IT Concept, Longessaigne, France. The time dependence of the surface tension was measured over a period ranging from 30 min to a few hours following the formation of the drop.

Results and Discussion

Self-Aggregation. The aggregation behavior of the cholesteryl-oligonucleotides in TBS was studied by means of fluorescence emission of a pyrene probe (Py), light scattering, and surface tension measurements.

Figure 2 reports the emission spectra of 1 μM pyrene, added to MC-ON$_1$ and SC-ON$_1$ solutions, for two cholesteryl-oligonucleotide concentrations (4 and 100 μM). The ratio of the intensities I_1/I_3 of Py fluorescence emission, determined from the first (372 nm) and the third (382 nm) vibronic peaks of the emission spectrum, decreases as the environment becomes more hydrophobic. For a given cholesteryl-oligonucleotide concentration, Py senses on average a more hydrophobic environment in MC-ON$_1$ solutions than SC-ON$_1$ systems.

From the I_1/I_3 ratio plotted against the cholesteryl-oligonucleotide concentration, we estimated the concentration which marks the onset of aggregation for MC-ON$_1$ and SC-ON$_1$, revealed by the decrease of the I_1/I_3 ratio, as shown in Figure 3. At 4 μM, SC-ON$_1$ is still in a nonaggregated form, whereas MC-ON$_1$ molecules already self-aggregate. At 100 μM the decreased ratio I_1/I_3 for SC-ON$_1$ reveals that the microenvironment around Py is more hydrophobic than that pertaining to bulk aqueous solution, and the SC-ON$_1$ self-aggregation concentration threshold has been exceeded. The CAC (critical aggregation concentration) determined from the onset of I_1/I_3 decrease is about 0.2 μM for MC-ON$_1$ and 10 μM for SC-ON$_1$. These threshold concentrations for aggregation differ by 1 order of magnitude.

Cholesterol has a maximum solubility in aqueous solutions of 1.8 mg/mL or 4.7 μM. It undergoes a thermodynamically reversible self-association with a critical micelle concentration of 25−40 nM at room temperature.[24] On the basis of very simple arguments and modeling aggregation as a pseudoseparation of phase, one obtains

$$\Delta G^0_{transf} \approx RT \ln X_{CAC} = -52 \text{ kJ mol}^{-1} \quad (4)$$

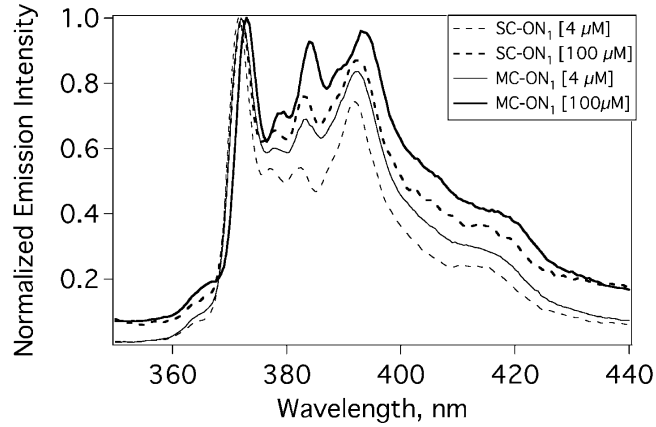

Figure 2. Py/cholesteryl-oligonucleotide normalized emission spectra (with respect to I_1 intensity) for two MC-ON$_1$ and SC-ON$_1$ concentrations (4 and 100 μM). Py is 1 μM in all samples.

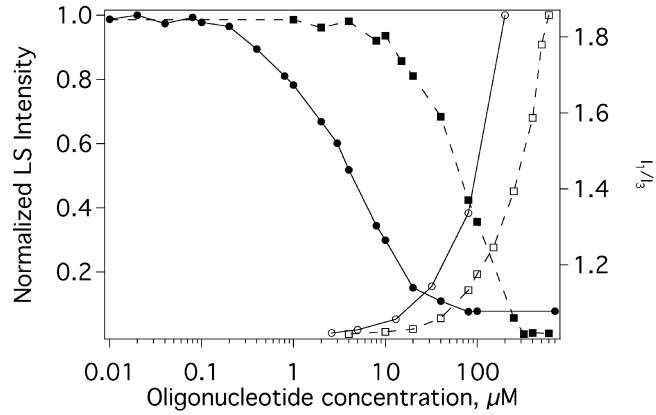

Figure 3. Py fluorescence intensity ratio I_1/I_3 and normalized light scattering intensity for MC-ON$_1$ (●, ○) and SC-ON$_1$ (■, □) as a function of cholesteryl-oligonucleotide concentration.

where ΔG_{transf} is the energy gain involved in the transfer of one mole of cholesterol units from water to the aggregate and X_{CAC} is the mole fraction corresponding to the critical aggregation concentration. At the experimental value of 10 μM for SC-ON$_1$, we can roughly estimate the contribution per base opposing micellization to be around 0.8 kJ mol^{-1} (see Supporting Information).

Considering that MC-ON$_1$ has on average 3.5 cholesterol units and ten more bases where the additional cholesteryl units are appended, ΔG^0_{transf} would be around −150 kJ mol^{-1} (see Supporting Information section for additional details), leading to a lowering of several orders of magnitude of the aggregation threshold. Even if coarse-grained, and completely neglecting the oxyethylene portions, these considerations indicate that the monomer MC-ON$_1$ should be virtually never observable with ordinary methods. The fact that this species is indeed detected (both indirectly, with fluorescent probe techniques, and directly, through light scattering, vide infra) is indicative of a more complex aggregation pattern than for the single-cholesterol derivative, namely, that the presence of several rigid fused-ring structures attached on the hydrophilic T segment might prevent complete segregation of the hydrophobic regions.

The fluorescence results can be correlated with the static light scattering data, as shown in Figure 3, where the intensity of the light scattered at 90°, normalized for toluene scattering, is reported for MC-ON$_1$ and SC-ON$_1$. For low oligonucleotide-amphiphile concentrations the scattering intensity is indistinguishable from the aqueous buffer, while the increase in static

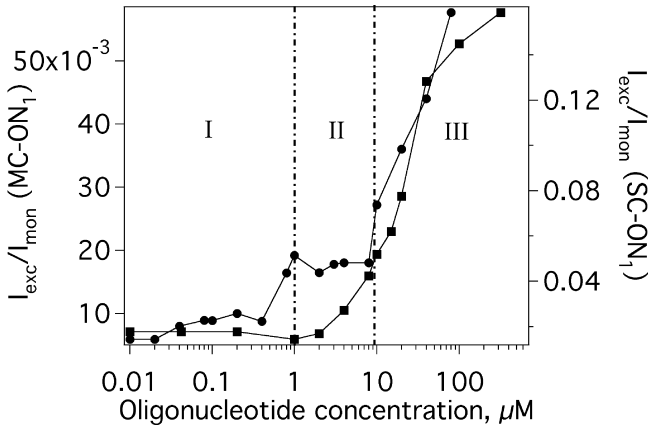

Figure 4. I_{exc}/I_{mon} ratios from 1 μM Py fluorescence spectra as a function of concentration for MC-ON$_1$ (●) and SC-ON$_1$ (■) in TBS. Three regimes of self-aggregation for MC-ON$_1$ species are indicated.

scattering reveals the occurrence of aggregates. In principle, the relatively large molecular size of oligonucleotide amphiphile unimers should allow their observation through light scattering. In practice, the extremely low number densities and weak optical contrast preclude the monitoring of unimers below the aggregation threshold. The intensity of scattered light is proportional to the squared volume of the scattering particles, and it is therefore a sensitive method to observe the onset of aggregation from unimers. For MC-ON$_1$, the scattered light intensity starts growing already at 5 μM concentration, whereas for SC-ON$_1$ it starts around 20 μM, which well correlate with the fluorescence probe data analysis.

The exact nature of these aggregates and of the aggregation process itself cannot be deduced from the shape of these curves, even if the presence of a concentration threshold is evident.

Classical mean field theories on amphiphilc self-assembly[25] predict that above this critical concentration value amphiphiles cooperatively aggregate thanks to hydrophobic effects in micelles with a more or less narrow size distribution. In our case the presence of one or more cholesteryl functions, which are quite rigid hydrophobic moieties, might direct aggregation in a fashion reminiscent of the well-known bile salt assembly: bile salts self-associate in water in small primary aggregates which increase as a function of concentration to form larger secondary aggregates[26] whose size and number increase as a function of concentration.[27] The behavior of I_1/I_3 as a function of MC-ON$_1$ and SC-ON$_1$ concentration shows a slow rather than a steep decrease for concentration higher than the CAC, typical of a multistep process, such as the bile salt systems.

More information on possible differences between the two derivatives can be obtained by a careful inspection of Py emission spectra above the CAC (see Supporting Information). The appearance of a broad band, centered around 480 nm and characteristic of Py excimers, is due the simultaneous presence of more than one Py molecule per pseudomicellar assembly, which is possible due to micellar growth. If the ratio of the excimer to the monomer fluorescence intensity, I_{exc}/I_{mon}, is plotted against the oligonucleotide concentration (Figure 4, where I_{exc} and I_{mon} are the fluorescent intensities at 480 and 394 nm, respectively), respectively, we notice that this quantity ratio is almost zero below the onset of cholesteryl-oligonucleotides aggregation and increases as the aggregates start forming. For SC-ON$_1$, the I_{exc}/I_{mon} ratio progressively increases along a continuous trend that can be associated to a gradual growth, while for MC-ON$_1$, I_{exc}/I_{mon} slightly increases first and then levels off in the range 1−10 μM of MC-ON$_1$ concentration. Within this concentration range, the ratio I_1/I_3 keeps decreasing (see Figure 3), thus indicating that more and more fluorescent probes are confined in the aggregates. Since I_{exc}/I_{mon} is constant in the same concentration range, the size of the aggregates is not increasing, but rather their number increases. Above 10 μM MC-ON$_1$ concentration, I_{exc}/I_{mon} shows a steep increase, as an effect of the increased size of the aggregates.

Surface tension was also used to gather information about the differences between the aggregation properties of the two derivatives. Cholesteryl-oligonucleotides are amphiphilic macromolecules which can decrease the surface tension of water through their adsorption at the air−water interface. It has been already shown elsewhere that DNA-based surfactants are surface active and can spontaneously adsorb both to the air−water and oil−water interface.[9]

Air−water dynamic surface tension (DST) measurements were performed at various concentrations of SC-ON$_1$ and MC-ON$_1$ in TBS (see Supporting Information), and equilibrium surface tension values were extrapolated from the curves at very long times of adsorption (4 h). Similar bulk concentrations for the two derivatives correspond to different concentration regimes with respect to the CAC: for SC-ON$_1$, we have explored a molarity range below and above the aggregation threshold, while for MC-ON$_1$, only solutions above aggregation (as revealed by SLS and Py fluorescence) could be investigated. Different equilibrium surface tension values were found for a given bulk concentration, the multicholesteryl species showing higher amphipathicity for all the molarities tested. Some differences in trends of the equilibrium values can be observed: while for SC-ON$_1$, surface tension is monotonously decreasing and does not show any obvious discontinuity, even if the onset of aggregation is in this concentration range, in the case of the multicholesterol derivative there is a region (1 order of magnitude in concentration, where aggregates are present) where γ is more or less invariant. However, for higher concentrations (above 20 μM), we observe a definite decrease in γ, corresponding to an increase in the surface concentration of the amphiphile. In this range of concentration, secondary aggregates, possibly with different sizes and shapes with respect to the previous regime, are present in solution and contribute to the increase in the surface concentration of MC-ON$_1$.

Remarkably, this invariance concentration range closely resembles the domain where I_{exc}/I_{mon} is invariant, which we have attributed to an increase in aggregate number density, without appreciable size increase. Moreover, from 20 μM on, the clear decrease of surface tension could indicate the presence of surface active aggregates, which can adsorb at the interface through hydrophobic dangling ends.

We have previously studied with DLS the structural properties of aggregates from SC-ON$_1$ in solution between 5 and 200 μM, obtaining an estimate of the hydrodynamic sizes for the unimer and the aggregate species.[10] We now focus on the comparison of SC-ON$_1$ assemblies with the MC-ON$_1$ aggregates, as obtained through DLS experiments for the two derivatives at a concentration of 80 μM, where MC-ON$_1$ shows a peculiar surface tension behavior (see Figure 5).

DLS autocorrelation functions, reported in Figure 6, show that for the single-cholesterol species we have an overall faster relaxation rate with respect to MC-ON$_1$, whose decay can be well accounted for by a biexponential function. For SC-ON$_1$ at this concentration, a monomodal decay distribution with some degree of polydispersity provides a good fit, while for higher concentrations a biexponential analysis of the DLS functions is required as well (Supporting Information), yielding the

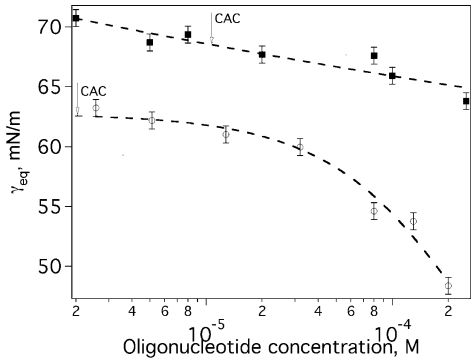

Figure 5. Equilibrium surface tension values calculated from the dynamic curves at different MC-ON_1 and SC-ON_1 concentrations.

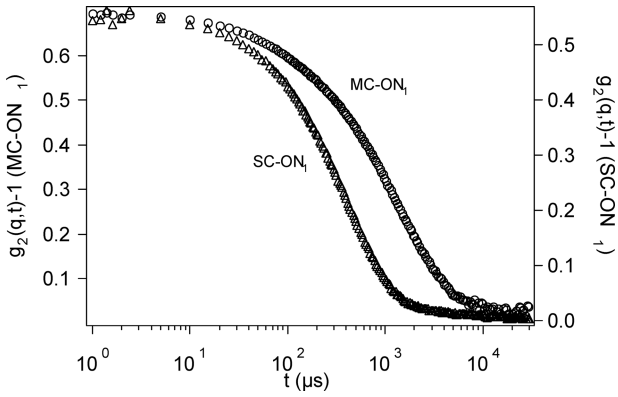

Figure 6. DLS autocorrelation functions at 90° for MC-ON_1 (circles) and SC-ON_1 (triangles); concentration of the two species is 80 μM.

diffusion coefficients both of the SC-ON_1 unimers/oligomers and of the aggregate.

By measuring the DLS functions at different scattering angles (at least 15 angles in our case, see Supporting Information), the corresponding apparent diffusion coefficients D can be extracted from the slope of the curve Γ (s^{-1}) versus q^2 (cm^{-2}). The calculated diffusion coefficients at 80 μM are $D_1 = 2.79 \times 10^{-7}$ cm^2/s and $D_2 = 1.88 \times 10^{-8}$ cm^2 s^{-1}, respectively, for the fast and the slow mode in the multiple-cholesterol system, while an average of $D = 5.27 \times 10^{-8}$ cm^2/s is obtained for the single relaxation mode in the single-cholesterol system, probably due to the fact that the unimer and the aggregate-like structures are not sufficiently different in sizes and their contribution to the autocorrelation function decay cannot be separated. When the SC-ON_1 concentration is increased, the aggregate size increases, and it is possible to separate the contribution of the unimer from the oligomer species, obtaining for 700 μM $R_{h1} =$ 7.9 nm for the unimer ($D_1 = 3.1 \times 10^{-7}$ cm^2/s) and $R_{h2} = 57.1$ nm for the aggregated species ($D_2 = 4.3 \times 10^{-8}$ cm^2/s).

The apparent diffusion coefficients calculated from DLS analysis for SC-ON_1 and MC-ON_1 unimers, $D_1 = 3.1 \times 10^{-7}$ and 2.79×10^{-7} cm^2/s, respectively, are in reasonable agreement with the theoretical values for the diffusion coefficients obtained with the HYDROPRO program,[28] introduced in the accompanying paper (9.8×10^{-7} cm^2/s for SC-ON_1 and 6.53×10^{-7} cm^2/s for MC-ON_1). The systematically lower experimental values are accounted for by the inclusion of water molecules in the extended hydrophilic shell of the oligonucleotide or by the presence of small oligomers.

The results obtained through pyrene probe fluorescence highlight that the aggregation of MC-ON_1 is a multistep process occurring in the concentration range 0.2−100 μM. The small primary aggregates (unimers or dimers) form first, and then they

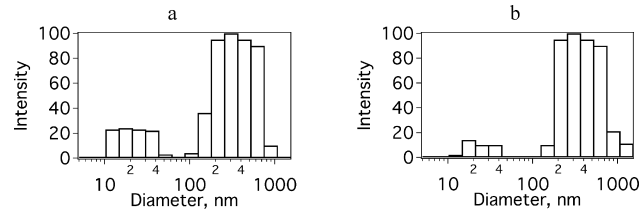

Figure 7. Apparent hydrodynamic diameter distribution functions calculated by CONTIN analysis method at 90° for two different MC-ON_1 concentrations: (a) 5 μM and (b) 80 μM.

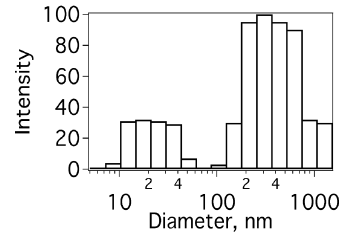

Figure 8. Apparent hydrodynamic diameter distribution functions calculated by the CONTIN analysis method at 90° for 80 μM MC-ON_1/ON_2FAM.

self-associate into larger secondary aggregates as the concentration of MC-ON_1 is increased.

Figure 7 reports the intensity-weighed apparent hydrodynamic diameter distributions obtained with the CONTIN algorithm at 5 and 80 μM of MC-ON_1. In both cases two well-separated populations occur, where the amplitude of the slow mode (i.e., larger hydrodynamic diameter) is dominant. The obtained hydrodynamic sizes ($<r_{h1}> \approx$ 12 nm and the second $<r_{h2}> \approx$ 180 nm) are consistent with those obtained with the simpler biexponential analysis, demonstrating the reliability of the former approach.

From the amplitude of the intensity-weighed size distribution, it is not possible to estimate the relative number of smaller and larger aggregates in solution, without any assumptions on the shape of the scattering particles.[29] However, we can say that the percentage of unimers or small oligomers, whose size distribution is centered at ≈25 nm, is higher for the lowest MC-ON_1 concentration (5 μM) than for 80 μM. The larger size population is centered around 300−400 nm, and it is slightly shifted to higher values when the concentration is increased to 80 μM. In this concentration range the isolated molecules are well distinguished from the aggregates: the amount of unimers/dimers progressively decreases and promotes the formation of larger aggregates, whose size and number increase as a function of concentration.

A noticeable result, which is peculiar to the multicholesterol oligonucleotide, was obtained through DLS experiments on the hybrid system ds-MC-ON_1, formed by 1:1 coupling of MC-ON_1 with the complementary ON_2 in solution. Figure 8 compares the CONTIN size distributions obtained for the 80 μM ss and ds samples, showing that the presence of two populations persists upon coupling.

A double exponential analysis of the autocorrelation functions yields similar results, though polydispersity is neglected. The apparent diffusion coefficients for the smaller scattering particles are 2.79×10^{-7} cm^2/s for the ss-MC-ON_1 and 1.96×10^{-7} cm^2/s for the ds-MC-ON_1 system. At 80 μM, ss-MC-ON_1 shows a population of small objects (unimers/dimers of MC-ON_1) with an average diameter centered at 25 nm. At the same concentration of ds-MC-ON_1, the population of small objects has a lower apparent diffusion coefficient, corresponding to a mean apparent

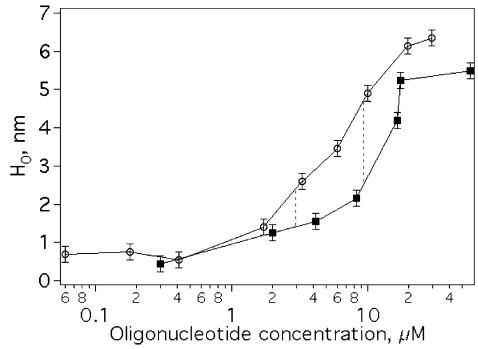

Figure 9. Hydrodynamic thickness around the vesicles upon oligonucleotide insertion for different oligonucleotide concentrations of MC-ON_1 (○) and SC-ON_1 (■).

hydrodynamic diameter of <35 nm, consistent with the duplex form of MC-ON_1. The theoretical values evaluated by means of HYDROPRO calculations are in accordance with these results (6.53×10^{-7} cm^2/s for the ss-MC-ON_1 and 6.43×10^{-7} cm^2/s for the ds-MC-ON_1). The slow relaxation mode of ds-MC-ON_1 is not particulaly affected by the hybridization.

The result of CONTIN, shown in Figure 8, is useful to understand the influence of hybridization on the different relative abundance of unimers/dimers and aggregates in solution. The amplitude of the smaller size population of scattering objects in the hybrid ds-MC-ON_1 system is consistent with a larger amount of structures if compared with the same distribution of scattering particles in the ss-MC-ON_1 system at the same molar concentration of oligonucleotides. The hybridization of MC-ON_1 molecules with complementary oligonucleotide is therefore competitive with a self-aggregation process, hence altering the unimer/aggregate ratio with respect to the pure MC-ON_1.

Insertion into POPC Vesicles. Vesicles decorated with MC-ON_1 lipophilic oligonucleotides have been obtained by dilution of POPC vesicles with TBS containing the amphiphilic oligonucleotide at different concentrations. In these experimental conditions, the scattering from MC-ON_1 self-aggregates is negligible with respect to vesicle scattering, and the decay of autocorrelation intensity is therefore due to Brownian motions of POPC/DNA hybrids. The variation of hydrodynamic sizes of the DNA-decorated POPC vesicles was determined through a cumulant fit of the DLS autocorrelation functions arrested at the second order. No appreciable variation of the polydispersity was noticeable throughout the concentration range explored, ruling out any DNA-mediated fusion events. The size progression observed is entirely due to an increase of hydrodynamic thickness as the hydrophobic oligonucleotides are partitioned in the membrane.

Upon insertion of SC-ON_1 into the vesicle membrane, the oligonucleotide portion together with the oligoethylene spacer protrudes outward from the membrane, causing an increase of hydrodynamic radius of the vesicles. In the same way, after the insertion of the multiple cholesterol-oligonucleotides, we observe a hydrodynamic thickness increase corresponding to an increase of the hydrodynamic radius of the POPC/DNA hybrids. However, some meaningful differences emerge for the two derivatives.

The increase in hydrodynamic thickness, termed H_0, is reported as a function of the oligonucleotide concentration in Figure 9 for MC-ON_1 and SC-ON_1. For the low oligonucleotide concentration range, below 2 μM, similar thicknesses result for the two systems, 0.5−0.6 nm at 0.3−0.4 μM oligonucleotide concentration and 1.0−1.2 nm at 2 μM. For higher concentrations, between 2 and 20 μM, we observe a steep increase of H_0 for the MC-ON_1/vesicle hybrids, whereas the values for SC-ON_1 increase more gradually. It is important to underline that for MC-ON_1 aggregates are present in solution already at these concentrations (mainly as small oligomers). Above 20 μM the hydrodynamic thickness seems to become level for SC-ON_1/vesicles and to a lesser extent for MC-ON_1/vesicles.

According to a previous work,[10] the correlation between the hydrodynamic thickness on the vesicles and the grafting density of the anchored single-cholesterol oligonucleotides can be referred to a conformational transition of the hydrophilic portion of the lipid-oligonucleotide. The average noncovalent grafting density can be reliably estimated, as the partition of the hydrophobic oligonucleotide is quantitative within experimental uncertainty in this concentration range, as demonstrated by gel exclusion chromatography. When the average distance between the oligonucleotides approaches the Flory radius, the chains are in a brush state, and the hydrodynamic thickness reaches its limiting value at the maximum membrane hosting capacity. In this surface density regime, which closely matches the monolayer saturation regime observed with QCM-Z for SLB, the average distance between SC-ON_1 is 5 nm.

When multiple cholesteryl anchors are present, the variation of the hydrodynamic thickness on the vesicles may not be as simply correlated to a conformational transition of the oligonucleotides protruding out of the membrane. Above 3 μM the hydrodynamic thickness for the anchored MC-ON_1 is 1 nm higher than the corresponding SC-ON_1 system, and this difference is maintained irrespective of concentration. This threshold is in the concentration range where MC-ON_1 aggregates are surface active (see Figure 5), possibly due to an incomplete segregation of the cholesteryl moieties inside the hydrophobic core, already predictable from the particularly high CAC values for this derivative. The affinity of the aggregates for the a/w interface can be correlated with partition in vesicles with respect to solution, meaning that the aggregates themselves can insert in membranes through the dangling cholesteryl units. According to these considerations, the inclusion in lipid bilayer membranes proceeds mediated by either unimer or aggregate insertion, and the increase of hydrodynamic radius is the result of these different processes occurring in different concentration ranges.

The apparent agreement of the vesicle hosting capacity and of the limiting hydrodynamic thickness of SC-ON_1 and MC-ON_1 might lead to incorrect conclusions about an overall structural and functional similarity for the two derivatives. In fact at the hosting capacity limit, the situation at the vesicle surface might be completely different, and the conformation (schematically represented in Figure 10), the aggregational state, and the availability of the coupling unit to build arrays of higher hierarchy might be dramatically altered.

A combined discussion of these DLS findings and QCM-Z results (see for instance Figure 6 of the accompanying paper) can shed some light into this particular aspect. With respect to these latter measurements, we are exploring POPC/MC-ON_1 ratios that correspond to the monolayer saturation regime, but the bulk concentration range is shifted more than 1 order of magnitude. Therefore, in DLS experiments, depending on the bulk concentration, either unimers or aggregates are in equilibrium with vesicles, while for QCM-Z experiments, only unimers are expected in bulk solution.

From the DLS picture, a reasonable hypothesis is that, while for SC-ON_1 partition is unimer-mediated, for MC-ON_1 in the presence of aggregates the insertion proceeds through aggregate insertion as well, thanks to the presence of hydrophobic anchors

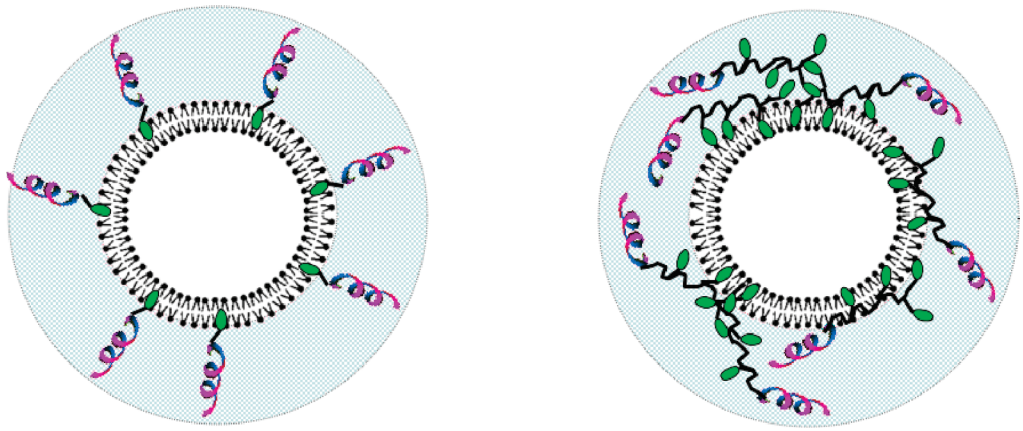

Figure 10. Possible oligonucleotide conformations for high grafting density on vesicles, SC-ON_1 (on the left) and MC-ON_1 (on the right).

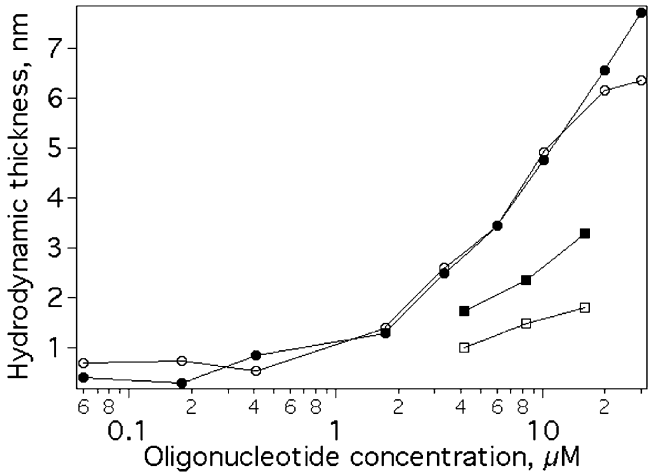

Figure 11. Hydrodynamic thickness around the vesicles versus oligonucleotide concentration upon cholesteryl-oligonucleotides insertion and further hybridization with complementary oligonucleotide: MC-ON_1 (○), SC-ON_1 (□), MC-ON_1/ON_2 (●), SC-ON_1/ON_2 (■).

dangling out from the aggregate. Therefore, the increase of the hydrodynamic thickness cannot be explained in terms of conformational transitions of isolated coils until the bilayer saturation is achieved but rather on the basis of a mixed mechanism where both unimers and aggregates contribute to vesicle decoration.

Hybridization at the Vesicle Surface. In view of the previous results, it is interesting to monitor the coupling process of DNA-decorated vesicles with the soluble complementary strands in solution. Classical UV methods and dynamic light scattering provide complementary information that can be related to molecular-level properties and structural modulation at the mesoscopic size, respectively. DLS has been used previously as a powerful and sensitive probe of hybridization on DNA-functionalized colloidal particles, such as gold nanoparticles.[30] In those systems, duplex formation on the surface of the nanoparticles leads to an increase in hydrodynamic radius, while duplex disassembly is characterized by a drop in hydrodynamic radius with increasing temperature.

Figure 11 compares the thickness of the hydrodynamic layer on POPC vesicles obtained by inclusion of the cholesteryl-oligonucleotides, together with the effect of further addition at room temperature of the complementary oligonucleotide in a 1:1 ratio. Hybridization leads to an increase of ≈2 nm in hydrodynamic diameter in the SC-ON_1/vesicle system, for the three different oligonucleotide concentrations tested. Linear dichroism of the DNA-decorated vesicles under shear high-

TABLE 1: UV Melting Data for ON_1-ON_2 in SC-ON_1 and MC-ON_1 Systems (1.1 μM)

	T_m [°C] (hyperchromicity %)	
	SC-ON_1	MC-ON_1
solution	48.6 ± 0.1 (24 ± 5)	47.2 ± 0.1 (20 ± 4)
vesicle	48.3 ± 0.1 (19 ± 4)	47.6 ± 0.1 (20 ± 4)

lighted for this system shows an increase of the tilt angle between the helix axis and the bilayer plane. The increase in hydrodynamic thickness is then due to a variation of the conformational and bending properties of the duplex with respect to the single strand.

MC-ON_1 hybridization at the vesicular surface with complementary ON_2 (in 1:1 ratio), investigated for a relatively large range of ON concentrations (0.6−30 μM), surprisingly does not determine any further increase in the hydrodynamic radius of the decorated vesicles. An analogous result has been also found on SLB by means of QCM-Z measurements, where the thickness of the adsorbed layer of MC-ON_1 molecules on the membrane is not varying upon the addition of the complementary strand in solution, while an increase in the adsorbed mass is registered.

The results on vesicles agree therefore with SLBs, showing that the curvature has a negligible effect on the structural properties of the hybrid and that the most important parameter is the molecular architecture of the hydrophobic part, which in turn determines the aggregative pattern in solution.

The different hydrophobic substitutions do not appreciably alter the pairing energetics, as indicated by the similar melting temperatures (see Table 1). Aggregation has also a scarce influence on strand disassembly since melting temperatures are close for unimer/complementary strand and aggregates/complementary strand. Remarkably, also the pairing yield is similar for both derivatives, as indicated by the close values of hyperchromicity, and the inclusion in bilayers does not affect this trend.

The possible presence of MC-ON_1 clusters on the vesicular surface does not affect their coupling, as it emerges from UV melting. MC-ON_1 has also been tested for a higher concentration (4.1 μM), evidencing no clear dependence of the melting temperature from concentration. Unfortunately, it is not possible to perform the melting experiment at even higher concentrations, due to the high molar absorbtivity of the oligonucleotides.

Decoration with Amphiphilic DNA: Vesicles versus Supported Lipid Bilayers. This chapter summarizes and compares the results obtained with the two oligo-derivatives in vesicles and SLB.

The self-association properties of both hydrophobic oligonucleotides have been monitored in solution by static light scattering and fluorescent probe emission. The aggregation threshold, as monitored through Py emission and confirmed by light scattering, starts around 10 μM for SC-ON$_1$ and at 0.2 μM for MC-ON$_1$. For both derivatives, aggregation is not a single-step cooperative process but rather consists of a gradual multistep association of unimers and/or oligomers into large aggregates. Simple considerations about the CAC of the two derivatives suggest that MC-ON$_1$ should have a much lower aggregation threshold, if all the cholesteryl moieties were segregated from water contact upon aggregation. Beyond the aggregation threshold, the excimeric emission of Py reveals a peculiar behavior for the aggregates of MC-ON$_1$ and, namely, the occurrence of a concentration range (1−10 μM) where the number of the aggregates increases, while they do not grow in size. This concentration domain is characterized by surface tension invariance. Above 10 μM, there is a definite size growth, and a parallel increase in surface activity is monitored. Dynamic light scattering allows tracing the relative abundance of unimers and/or smaller oligomers for this derivative, as concentration is varied. The experimental hydrodynamic sizes for the smallest scattering objects are of the same order of magnitude but not identical to the theoretically estimated molecular sizes in vacuo, due to a predictably high hydration degree of the polar portion, to conformational variations driven by different affinity for the solvent of the hydrophobic and hydrophilic portions, or to formation of primary aggregates. The larger aggregates have high hydrodynamic sizes, consistent with asymmetric shapes with an elevated axial ratio. The overall picture is consistent with different concentration regimes for MC-ON$_1$: a pre-CAC region (<0.2 μM), where only unimers and small oligomers are present, an immediately post-CAC region (1−10 μM), where aggregates are relatively monodisperse, and a third concentration domain (>10 μM), where an extended growth occurs. Aggregation does not presumably result in complete segregation of the hydrophobic groups from the aqueous medium.

Cholesterol-conjugated oligonucleotides can be directly incorporated into lipid bilayers through spontaneous insertion of one or more cholesteryl moieties into the bilayer. Cholesterol embeds within the hydrophobic interior of the bilayer, forming a mobile anchor, while the hydrophilic spacer-oligonucleotide part protrudes outward from the membrane extending into the aqueous phase, and this is revealed by the formation of a hydrodynamic thickness around the vesicle in solution and an ad-layer thickness in SLBs. Apart from the obvious curvature difference for the two systems, two other important aspects should be taken into account, when comparing the results obtained for the oligo-derivatives in vesicles or supported lipid membranes: (i) The active area of the QCM-Z crystal coated with the bilayer is 78.5×10^{12} nm^2, while for vesicles the working concentration sets the total accessible area (external vesicular leaflet) at about 30×10^{19} nm^2. This of course shifts by several orders of magnitude the concentration ranges necessary to achieve a nominally identical lipid/guest ratio. (ii) The total phospholipid surface is different, not only quantitatively but also from a dynamical point of view. For liposomes, it consists of disconnected domains (the vesicles themselves), while for SLB there is a continuous, macroscopically extended bilayer domain. Therefore, any cooperative process may lead to different products also for an identical phospholipid/amphiphilic DNA ratio: this applies both to lateral interactions in the membrane and to membrane-induced processes at the lipid/aqueous interface. For example, the distribution of amphiphilic DNA molecules among the vesicles can be described by a Poisson distribution, which means that the probability of oligonucleotide occupancy $P(N)$ can be well approximated by a Gaussian distribution function centered at the mean value $\langle N \rangle$, with the assumption that events occur independently on each vesicle. The same does not occur on SLB, where the adsorption events for the amphiphilic DNA molecules at the membrane surface are not independent from each other.

SC-ON$_1$ inserts into the vesicular bilayer when the concentration of SC-ON$_1$ is $\leq$15 μM. In our experimental conditions, this threshold corresponds to a grafting density on the vesicle close to the Flory radius of the hydrophilic portion of the derivative, thus reinforcing the evidence that the hydrophobic oligonucleotide inserts as a unimer in the membrane. Above this limit, the liposome surface gets saturated, and the hydrodynamic thickness levels off.

The complementary investigation onto planar POPC bilayers performed using QCM-Z indicates a pseudo-Langmuir adsorption isotherm, and the bilayer saturation beyond a POPC/SC-ON$_1$ ratio is equal to 80. This value corresponds for vesicle solutions in our experimental conditions to SC-ON$_1$ concentrations of $\geq$10 μM, in agreement with the trend for the hydrodynamic radius. We can therefore interpret the leveling of the hydrodynamic thicknesses as the approach to the saturation threshold and a substantial similarity between the insertion patterns on curved and planar bilayer surfaces. Interestingly, the hydrodynamic thickness on the vesicle and the SLB adlayer thickness are strictly comparable, confirming that both systems are consistent with a unified picture.

A totally different picture emerges for MC-ON$_1$, both for the SLB and for vesicles: in the case of SLB, three clearly separated regimes occur and can be characterized in terms of adlayer thickness and viscoelasticity. The first regime results in monolayer saturation, not according to a simple Langmuir-type isotherm, but rather in a cooperative fashion, as demonstrated by the strong nearest-neighbor attraction strength parameter. This indicates that insertion is activated by the presence of guest molecules in the bilayer. The resulting limiting thickness (1.7 nm) is achieved on the vesicular surface for 400 lipid molecules/MC-ON$_1$ corresponding to a concentration of MC-ON$_1$ = 2 μM, i.e., an area 10 times higher than that of SC-ON$_1$. The increase in vesicle hydrodynamic radii is not appreciably different for MC-ON$_1$ and SC-ON$_1$ below 2 μM, and QELS results indicate that both adsorb at the vesicular surface as unimers.

For [MC-ON$_1$] $\geq$2 μM, the hydrodynamic thickness around the vesicles is considerably higher than in the SC-ON$_1$ case. This behavior can be attributed to unimer adsorption onto already occupied sites on the bilayer surface or, alternatively, to the insertion of aggregates from solution that do not readily disassemble in the presence of bilayers. We should stress however that there is no time evolution of the hydrodynamic sizes (for one week at least) to indicate a transient state. The surface activity of the aggregates in this concentration range is consistent with the presence of cholesteryl dangling ends that can mediate aggregate insertion in the bilayer.

It is not possible to detect any size-invariant adsorption region corresponding to the size-invariance regime of the aggregates: this is likely due to the fact that as more aggregates are forced into close proximity on the vesicles different conformational features arise that cause a variation of the hydrodynamic thickness. We recall that in this concentation regime also SC-ON$_1$ molecules insert as isolated unimers and cause an increase of the hydrodynamic thickness, due to lateral repulsive interactions.

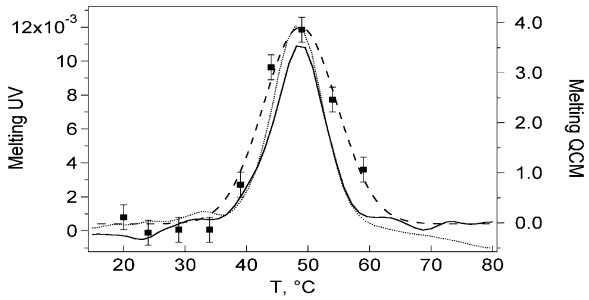

Figure 12. Normalized first derivative of MC-ON_1/ON_2 melting curves: UV−vis in solution (•••), UV−vis on SUV (—), QCM-Z onto SLB (■).

This can be better appreciated through QCM-Z, where, beyond the monolayer saturation, the other two regimes can be observed: in the second regime unimers might approach the surface in random orientation and be adsorbed either onto free spots or onto preexisting host patches; in the third one, the results indicate a clear membrane-assisted association mechanism that is likely to result in aggregate formation at the interface.

No membrane-driven aggregation can be observed for vesicles in correspondence of the same POPC/MC-ON_1 ratios: this is a very important result and introduces a noteworthy difference between SLB and liposomes. Though a combination of factors might contribute to this behavior, the effect of curvature should be, in our opinion, a minor determinant. More likely, two effects are simultaneously in action: one is the fact that SLB is a much more efficient reservoir for MC-ON_1 since virtually all the guest molecules are connected in a single bilayer, and thus a cooperative mechanism can produce very different results. The second effect is the fact that for vesicles both partners are undergoing Brownian motions in solution, and in the option of kinetically driven events, this might as well result in different behavior.

Hybridization of the membrane-anchored oligonucleotide with a complementary oligonucleotide occurs with a contraction of the base unimer length (from 4.3−7 Å for the ss-DNA to ≈3.4 Å for the ds-DNA), whereas the increased rigidity of the duplex increases the effective radius to the contour length.

In the case of SC-ON_1, in the regime of unimer adsorption at the vesicular membrane, the hybridization with the complementary ON_2 leads to an increase in the hydrodynamic thickness around the vesicles. For MC-ON_1, we do not observe any hydrodynamic thickness increase upon hybridization in the whole range of concentrations, as observed also for the in situ hybridization of MC-ON_1 onto planar SLB. Therefore, the adsorption of the duplex form MC-ON_1/ON_2 results in a compact packing of the double strand at the surface for both curved and planar, maintaining a flat lying orientation with respect to the bilayer.

UV melting experiments confirm that hybridization at the liposomal surface occurs and that the thermodynamic stability of the duplex anchored to the bilayer is the same as in solution for the two systems. The extent of hyperchromic effect related to the oligonucleotide melting is unchanged when the strands come apart on the lipid surface, meaning that the membrane anchoring does not alter the coupling properties of the oligonucleotide. Moreover, the hybridization is not influenced by the number of anchoring cholesteryl groups present in the molecule (see Figure 12).

The full width at half-maximum (fwhm) for the liposomal curve is slightly lower than in SLB, suggesting a more cooperative transition in the case of liposome anchoring. The heating−cooling scans have demonstrated that melting is fully reversible. Therefore, the lipid bilayer decoration with double strand oligonucleotides can be switched on and off thermally. This characteristic can be exploited in the design of complex architectures, composed of several complementary strands, by tailored programming of melting temperatures, which are closely and predictably correlated to the base sequence.

Conclusions

The results of the present work provide a paradigm for membrane insertion of amphiphilic DNA and may be relevant for the construction of responsive hierarchically organized nanostructures.

POPC membranes decorated by lipophilic DNA can be easily prepared through spontaneous assembly of cholesteryl-oligonucleotides with the lipid bilayer. Small unilamellar vesicles (35 nm radius) and planar supported lipid bilayers (SLB) made of POPC phospholipids are taken as model membrane host systems for a lipophilic 18-mer oligonucleotide. The proper choice of the anchoring function is demonstrated to be very important to get highly density addressable DNA/lipid structures with tunable properties and various performances. Thanks to a novel DNA synthetic strategy, ss-DNA carrying lipophilic nucleotides in different positions within the oligonucleotide chain is obtained. A multiple-cholesterol vs a single-cholesterol anchor parallel study is presented here: by varying the number of cholesteryl moieties in the lipophilic DNA, we observe that the adsorption mechanism to the membrane, the grafting density, the stability, and the orientation of the inserted oligonucleotide are significantly different. In particular, the major hydrophobicity of the multiple-cholesterol species is responsible for higher self-assembly properties determining a characteristic three-step mechanism of aggregation of the molecules in solution, which is reflected by a peculiar 3-fold cooperative adsorption mechanism to the lipid membrane. DNA grafting density and orientation of the oligonucleotide on the bilayer are investigated at different DNA concentrations, and they can be finely tuned by changing the anchoring groups: at low concentration, the DNA portion of the inserted multiple-cholesterol molecule is flat on the membrane, while for the single-cholesterol it is in a random coil conformation; at higher concentration, the multiple-cholesterol oligonucleotides form a compact dense structure of molecules that maintain a flat orientation on the surface, while the single-cholesterol oligonucleotides undergo a conformation transition to a brush state, where the DNA chain is extending outward from the bilayer.

Interestingly, the hybridization thermodynamics of the membrane-anchored oligonucleotide with a complementary sequence is not affected by the membrane; i.e., the stability of the double-stranded DNA is the same as in solution.

Curved and planar bilayes do not show differences concerning the anchoring properties and hybridization efficiency of the lipophilic oligonucleotide, but they can be used for different applications, such as formation of 3D networks of DNA-connected liposomes, nanolayered objects where DNA vesicles can be sequentially tethered to planar bilayers, platforms for protein and DNA sensing, or scaffolds for responsive addressable devices, etc.

The overall results provide a paradigm for membrane insertion of amphiphilic DNA and, more ambitiously, may be relevant for the construction of responsive hierarchically organized nanolayered objects where vesicles containing lipophilic DNA strands could be sequentially tethered to planar bilayers displaying oligonucleotides of complementary sequence.[31] Alterna-

tively, vesicles decorated with programmable DNA sequences may be driven to ordered 3D-aggregation by the programmable hybridization of oligonucleotides protruding in the surrounding solution. These flexible construction schemes would result in the formation of metastructures with unusual electronic and optical properties.

Acknowledgment. Financial support from CSGI, MIUR-PRIN 2008, CNR-FUSINT, and the European Commission's Sixth Framework Program (Project reference AMNA, contract no. 013575) is acknowledged.

Supporting Information Available: Calculation of Gibbs free energy for cholesteryl-oligonucleotide aggregation, fluorescence emission spectra of Pyrene/SC-ON_1 and Pyrene/MC-ON_1, dynamic surface tension results for the amphiphilic DNA, dynamic light scattering multiangle measurement analysis, and melting of the oligonucleotides by DLS measurements. This material is available free of charge via the Internet at http://pubs.acs.org.

References and Notes

(1) Feldkamp, U.; Niemeyer, C. M. *Angew. Chem., Int. Ed.* **2006**, *45*, 1856–1876.
(2) Rothemund, P. W. K. *Nature* **2006**, *440*, 297–302.
(3) Seeman, N. C. *Nature* **2003**, *421*, 427–431.
(4) Seeman, N. C. *Mol. Biotechnol.* **2007**, *37*, 246–257.
(5) Park, S. Y.; Lytton-Jean, A. K. R.; Lee, B.; Weigand, S.; Schatz, G. C.; Mirkin, C. A. *Nature* **2008**, *451*, 553–556.
(6) Nykypanchuk, D.; Maye, M. M.; van der Lelie, D.; Gang, O. *Nature* **2008**, *451*, 549–552.
(7) Yoshina-Ishii, C.; Boxer, S. G. *J. Am. Chem. Soc.* **2003**, *125*, 3696–3697.
(8) Benkoski, J.; Hook, F. *J. Phys. Chem. B* **2005**, *109*, 9773–9779.
(9) Xu, C.; Taylor, P.; Fletcher, P. D. I.; Paunov, V. N. *J. Mater. Chem.* **2005**, *15*, 394–402.
(10) Banchelli, M.; Betti, F.; Berti, D.; Caminati, G.; Bombelli Baldelli, F.; Brown, T.; Wilhelmsson, M.; Nordén, B.; Baglioni, P. *J. Phys. Chem. B* **2008**, *112*, 10942–10952.
(11) Chan Yee-Hong, M.; van Lengerich, B.; Boxer, S. G. *Proc. Natl. Acad. Sci. U.S.A.* **2009**, *106*, 979–984.
(12) Loew, M.; Kang, J.; Dahne, L.; Hendus-Altenburger, R.; Kaczmarek, O.; Liebscher, J.; Huster, D.; Ludwig, K.; Bottcher, C.; Herrmann, A.; Arbuzova, A. *Small* **2009**, *5*, 320–323.
(13) Beales, P. A.; Vanderlick, T. K. *J. Phys. Chem. B* **2009**, *113*, 13678–13686.
(14) Tumpane, J.; Sandin, P.; Kumar, R.; Powers, V. E. C.; Lundberg, E. P.; Gale, N.; Baglioni, P.; Lehn, J.-M.; Albinsson, B.; Lincoln, P.; Wilhelmsson, M.; Brown, T.; Nordén, B. *Chem. Phys. Lett.* **2007**, *440*, 125–129.
(15) Bombelli Baldelli, F.; Gambinossi, F.; Lagi, M.; Berti, D.; Caminati, G.; Brown, T.; Sciortino, F.; Nordén, B.; Baglioni, P. *J. Phys. Chem. B* **2008**, *112*, 15283–15294.
(16) Bombelli Baldelli, F.; Betti, F.; Gambinossi, F.; Berti, D.; Caminati, G.; Lagi, M.; Sciortino, F.; Brown, T.; Baglioni, P. *Soft Matter* **2009**, *5*, 1639–1645.
(17) Gissot, A.; Camplo, M.; Grinstaff, M. W.; Barthélémy, P. *Org. Biomol. Chem.* **2008**, *6*, 1324–1333.
(18) Gambinossi, F.; Banchelli, M.; Durand, A.; Berti, D.; Brown, T.; Caminati, G.; Baglioni, P. *J. Phys. Chem. B* **2010**, *114*, DOI: 10.1021/jp100730x.
(19) Gosse, C.; Boutorine, A.; Aujard, I.; Chami, M.; Kononov, A.; Cogné-Laage, E.; Allemand, J.-F.; Li, J.; Jullien, L. *J. Phys. Chem. B* **2004**, *108*, 6485–6497.
(20) Brown, T.; Grzybowski, J. *Gene Probes 1: A Practical Approach*; Oxford University Press: New York, 1995.
(21) Walde, P.; Ichikawa, S. *Biomol. Eng.* **2001**, *18*, 143–177.
(22) Bertolotti, S. G.; Zimerman, O. E.; Cosa, J. J.; Previtali, C. M. *J. Lumin.* **1993**, *55*, 105–113.
(23) Provencher, S. W. *Comput. Phys. Commun.* **1982**, *27*, 213–227.
(24) Haberland, M. E.; Reynolds, J. A. *Proc. Natl. Acad. Sci. U.S.A.* **1973**, *70*, 2313–2316.
(25) Gelbart, W. M.; Benshaul, A. *J. Phys. Chem.* **1996**, *100*, 13169–13189.
(26) Voinova, M. V.; Rodahl, M.; Jonson, M.; B, K. *Phys. Scr.* **1999**, *59*, 391–396.
(27) Bandey, H. L.; Martin, S. J.; Cernosek, R. W.; Hillman, A. R. *Anal. Chem.* **1999**, *71*, 2205–2214.
(28) De la Torre, J. G.; Huertas, M. L.; Carrasco, B. *Biophys. J.* **2000**, *78*, 719–730.
(29) Hallett, F. R.; Watton, J.; Krygsman, P. *Biophys. J.* **1991**, *59*, 357–362.
(30) Xu, J.; Craig, S. L. *J. Am. Chem. Soc.* **2005**, *127*, 13227–13231.
(31) Yoshina-Ishii, C.; Boxer, S. G. *J. Am. Chem. Soc.* **2003**, *125*, 3696–3697.

JP100731C